Supporting information

Highly adhesive chitosan/poly(vinyl alcohol) hydrogels via the synergy of phytic acid and boric acid and their application as highly sensitive and widely linear strain sensors

Cuiwen Liu, Ru Zhang, Yao Wang, Chengmeng Wei, Feng Li, Ning Qing, Liuyan Tang*

School of Biotechnology and Health Sciences, Wuyi University, Jiangmen, 529020, China

*Corresponding author.

E-mails: wyuchemtangly@126.com; tangly@wyu.edu.cn (Liuyan Tang)

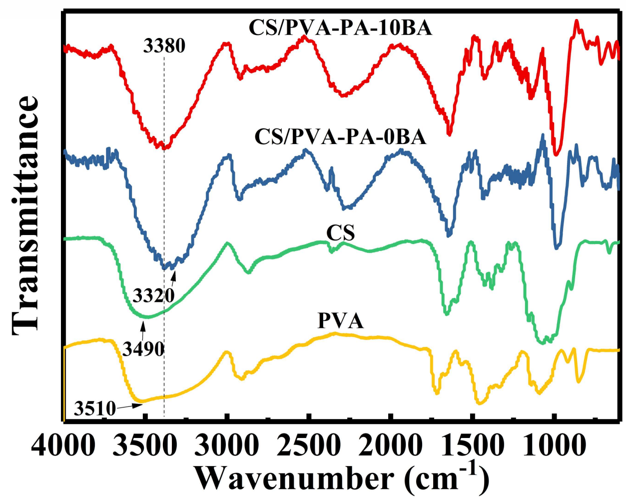

Fig. S1. FTIR spectra of CS/PVA-PA-10BA hydrogel, CS/PVA-PA-0BA hydrogel, CS and PVA with a highlight of the O-H and N-H bands.

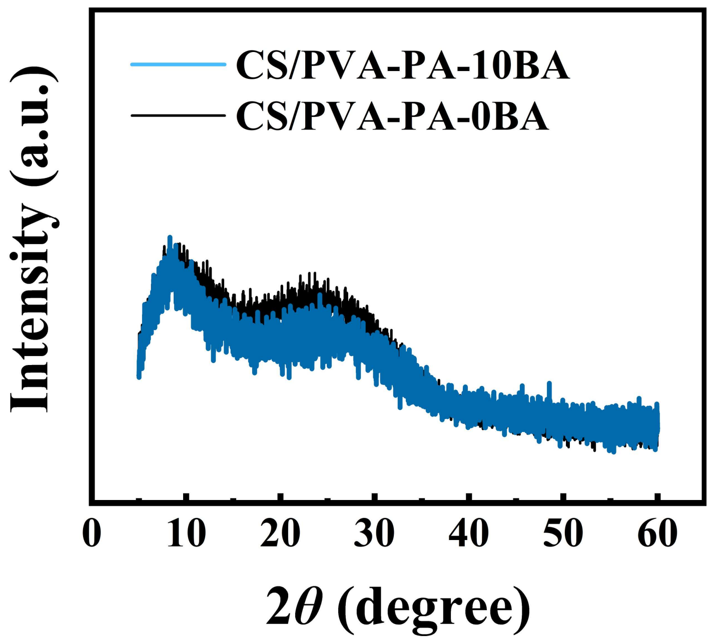

Fig. S2. XRD spectra of the CS/PVA-PA-0BA and CS/PVA-PA-10BA hydrogels.

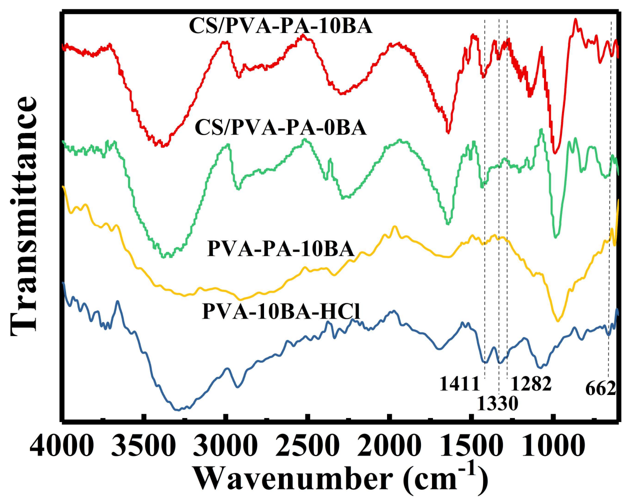

Fig. S3. FTIR spectra of the CS/PVA-PA-10BA, CS/PVA-PA-0BA, PVA-PA-10BA and PVA-10BA-HCl hydrogels.

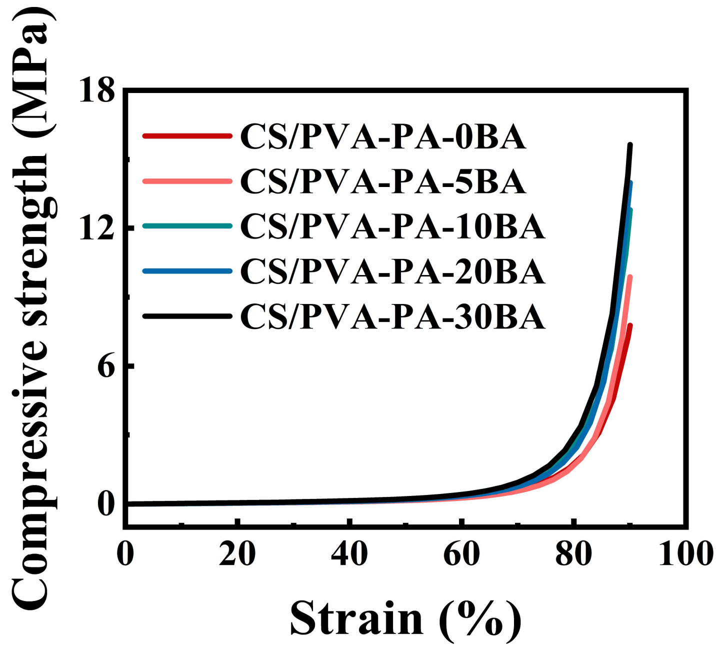

Fig. S4. Compressive stress-strain curves of CS/PVA-PA-BA hydrogels.

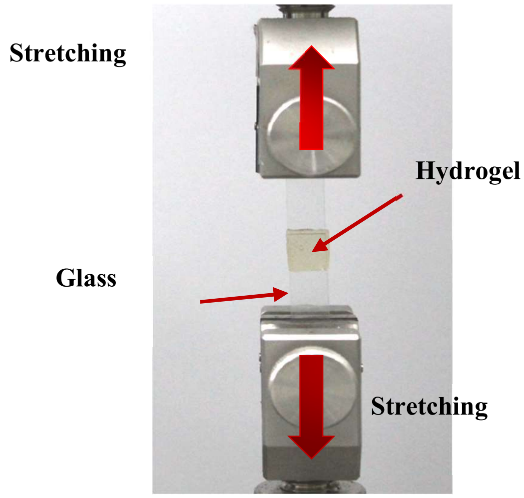

Fig. S5. Schematic illustration of the lap shear test.

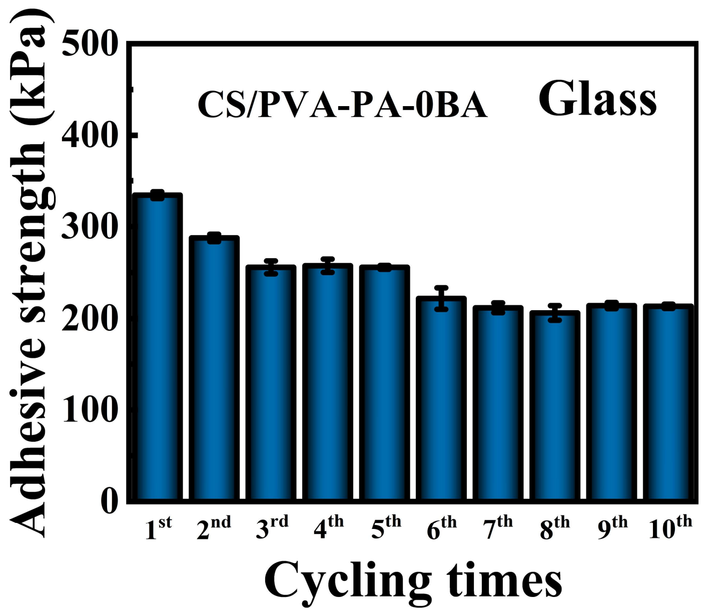

Fig. S6. Adhesive strength of CS/PVA-PA-0BA hydrogel under repeatedly bonding to glass substrates for 10 cycles.

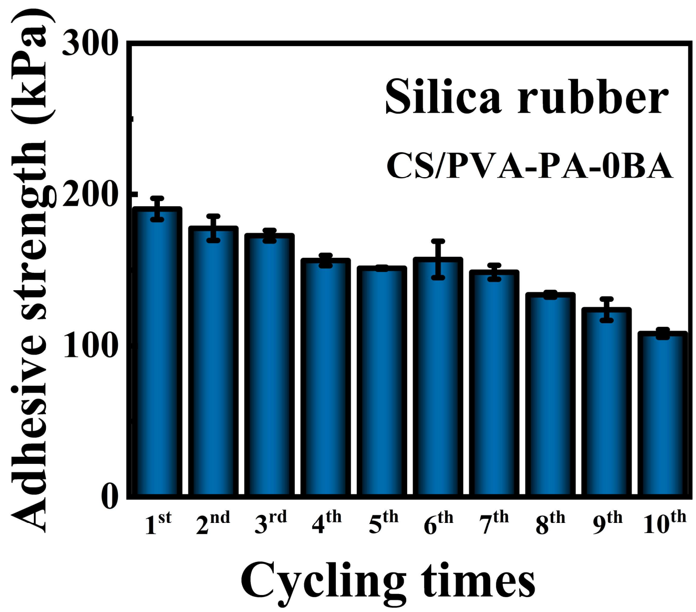

Fig. S7. Adhesive strength of CS/PVA-PA-0BA hydrogel under repeatedly bonding to silica rubber for 10 cycles.

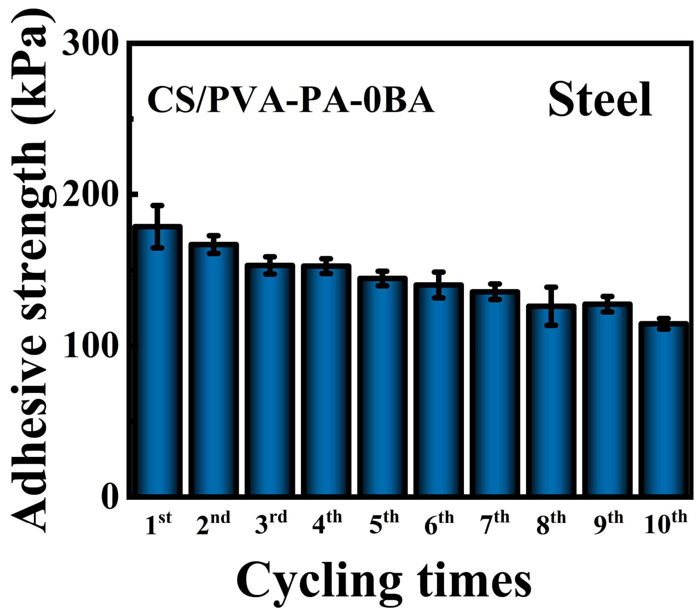

Fig. S8. Adhesive strength of CS/PVA-PA-0BA hydrogel under repeatedly bonding to steel substrates for 10 cycles.

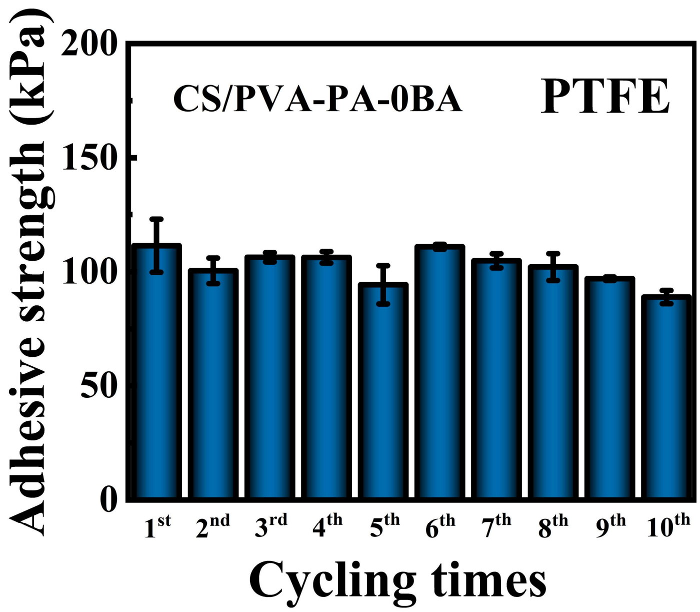

Fig. S9. Adhesive strength of CS/PVA-PA-0BA hydrogel under repeatedly bonding to PTFE substrates for 10 cycles.

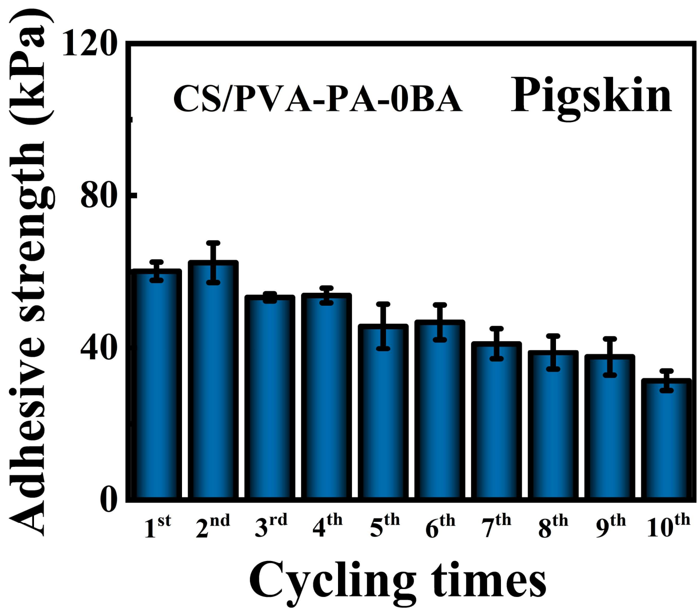

Fig. S10. Adhesive strength of CS/PVA-PA-0BA hydrogel under repeatedly bonding to pigskin for 10 cycles.

Fig. S11. Photographs of CS/PVA-PA-10BA hydrogel before and after adhering to the skin.

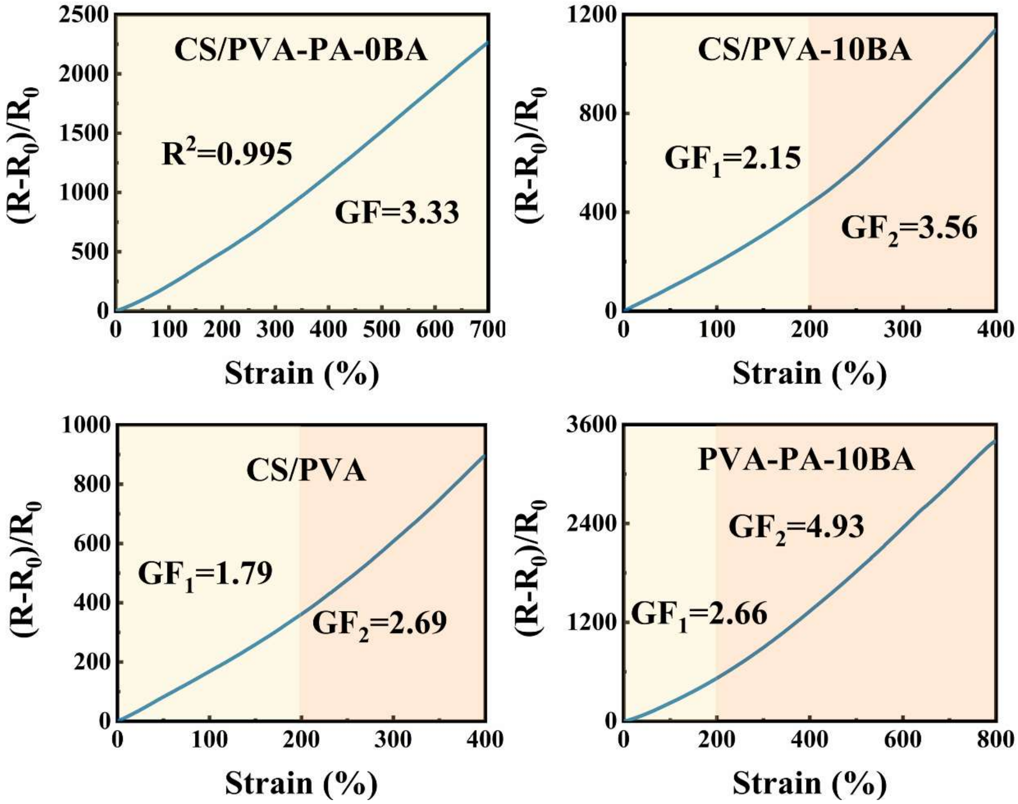

Fig. S12. Relative resistance changes and the GF of the strain sensors based on CS/PVA-PA-10BA, CS/PVA-PA-0BA, CS/PVA-10BA, CS/PVA, and PVA-PA-10BA hydrogels under various tensile strains.

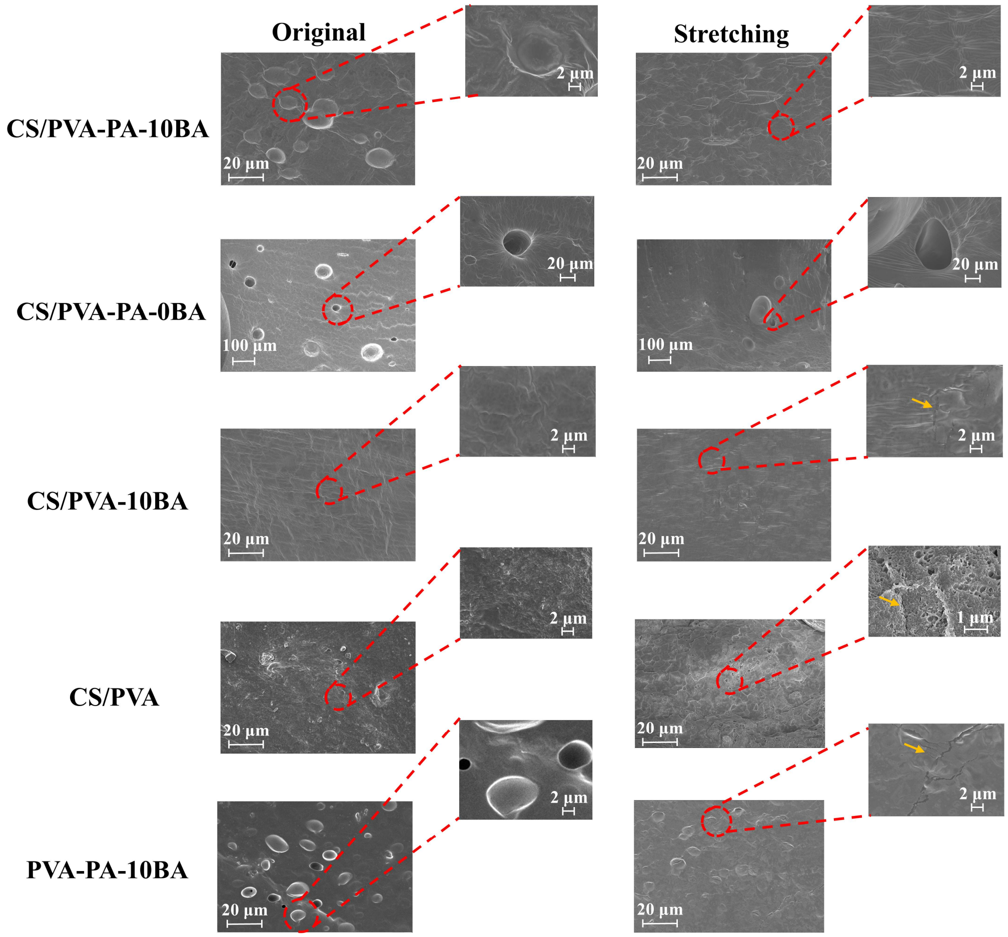

Fig. S13. SEM images of CS/PVA-PA-10BA, CS/PVA-PA-0BA, CS/PVA-10BA, CS/PVA, and PVA-PA-10BA hydrogels before and during stretching.

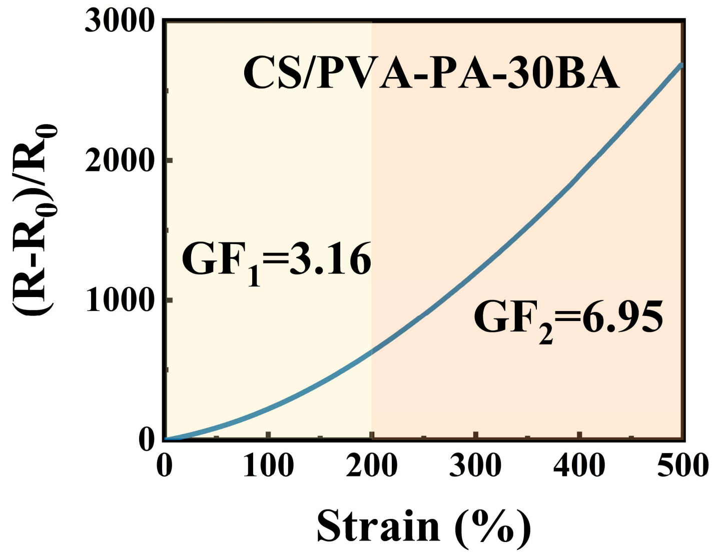

Fig. S14. Relative resistance changes and the GF of the strain sensors based on CS/PVA-PA-30BA hydrogel under various tensile strains.

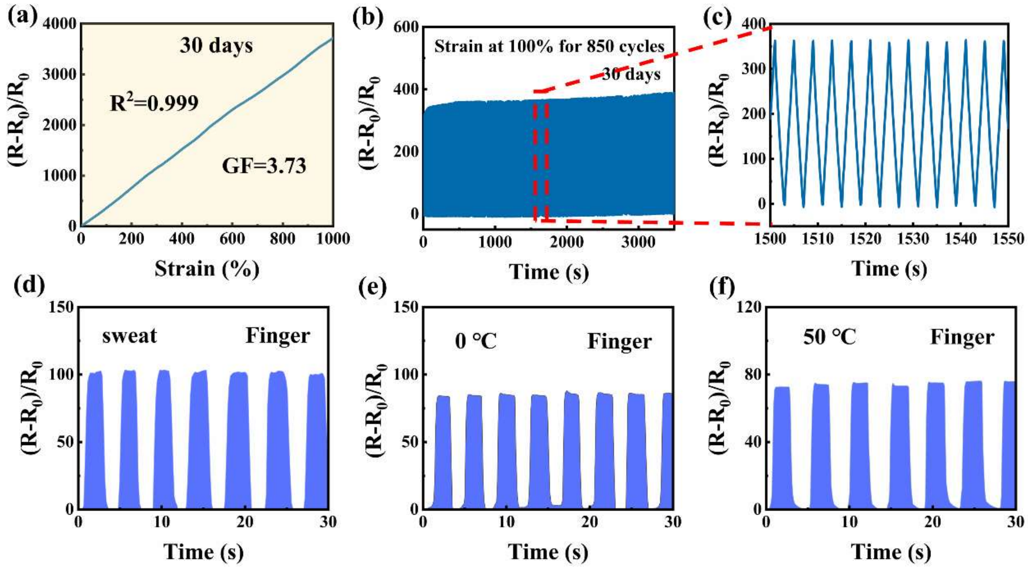

Fig. S15. The stability of CS/PVA-PA-10BA hydrogel-based strain sensor under different environmental conditions. (a) Relative resistance changes and the GF of the strain sensor under various tensile strains (0-1000%) after 30-day storage. (b) Relative resistance changes of the strain sensor under 850 loading-unloading cycles at 100% strain after 30-day storage. (c) A zoom-in view of the relative resistance changes from the loading-unloading cycles. Real-time monitoring of finger bending under (d) sweaty condition, (c) at 0 °C, and (d) at 50 °C.

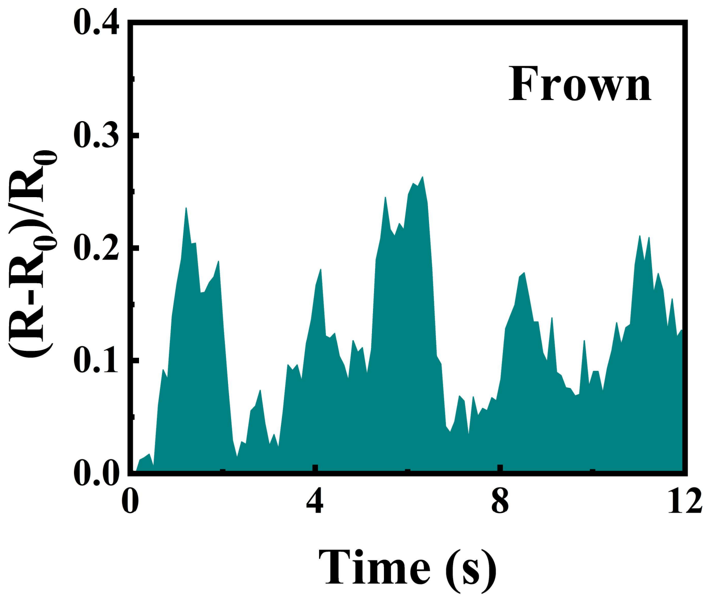

Fig. S16. Real-time monitoring of human frowning by CS/PVA-PA-10BA hydrogel-based strain sensor.

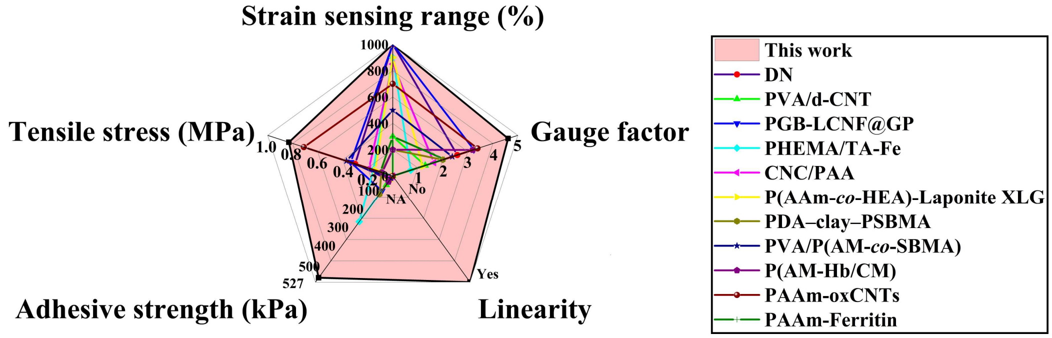

Fig. S17. Comparison of the tensile stress, adhesive strength, strain sensing range, gauge factor, and linearity between the strain sensor in this work and other strain sensors that have been reported previously.

Table S1. Comparison of the strain sensor in this work with other reported strain sensors.

Hydrogel	Tensile stress (MPa)	Adhesive strength (kPa)	Strain sensor range (%)	Linearity	Gauge factor	Ref
CS/PVA-PA-10PB	0.830	527	0-1000	Yes	4.61	This work
DN	0.300	20.87	0-450 500-1000	No	2.58 1.89	1
PVA/d-CNT	0.00068	45.6	0-100 100-175 175-300	No	1.08 1.04 1.30	2
PGB-LCNF@GP	0.336	76.8	0-500 500-1000	No	1.17 3.24	3
PHEMA/TA-Fe	0.155	238	0-500 500-900	No	0.55 0.72	4
CNC/PAA	0.190	3.1	0-65 65-470 470-850	No	0.57 1.03 1.65	5
P(AAm-co-HEA)-Laponite XLG	0.140	27.6	0-100 100-900	No	0.5 1.2	6
PDA–clay–PSBMA	0.090	94.3	0-80 80-200	No	1.25 2	7
PVA/P(AM-co-SBMA)	0.370	11.7	0-10 10-100 100-500	No	0.79 1.35 2.38	8
P(AM-Hb/CM)	0.085	30	0-110 110-200	No	0.9 3.2	9
PAAm-oxCNTs	0.71	NA	0-250 250-700	No	1.5 3.39	10
PAAm-Ferritin	0.099	NA	0-30 30-150 150-300	No	0.55 1.94 2.06	11

Table S2. The detailed compositions of the hydrogels.

Sample	PVA (g)	CS (g)	PA (mL)	H_2O (mL)	BA (g)	BA/H_2O (wt%)
CS/PVA-PA-0BA	1.50	0.30	4	1	0	0
CS/PVA-PA-5BA	1.50	0.30	4	1	0.05	5
CS/PVA-PA-10BA	1.50	0.30	4	1	0.1	10
CS/PVA-PA-20BA	1.50	0.30	4	1	0.2	20
CS/PVA-PA-30BA	1.50	0.30	4	1	0.3	30
CS/PVA	1.50	0.3	0	5	0	0
CS/PVA-2BA	1.50	0.3	0	5	0.1	2
PVA-PA-10BA	1.50	0	4	1	0.1	10
PVA-PA	1.50	0	5	0	0	0

References

1 H. Zhou, J. Lai, X. Jin, H. Liu, X. Li, W. Chen, A. Ma and X. Zhou, *Chem. Eng. J.*, 2021, **413**, 127544.

2 H. Zhu, J. Xu, X. Sun, Q. Guo, Q. Guo, M. Jiang, K. Wu, R. Cai and K. Qian, *J. Mater. Chem. A*, 2022, **10**, 23366–23374.

3 F. Lin, Y. Qiu, X. Zheng, Z. Duanmu, Q. Lu, B. Huang, L. Tang and B. Lu, *Chem. Eng. J.*, 2022, **437**, 135286.

4 F. Wang, C. Chen, J. Wang, Z. Xu, F. Shi and N. Chen, *Colloids Surfaces A Physicochem. Eng. Asp.*, 2023, **658**, 130591.

5 W. Ma, W. Cao, T. Lu, Z. Jiang, R. Xiong, S. K. Samal and C. Huang, *ACS Appl. Mater. Interfaces*, 2021, **13**, 58048–58058.

6 Z. He and W. Yuan, *ACS Appl. Mater. Interfaces*, 2021, **13**, 53055–53066.

7 X. Pei, H. Zhang, Y. Zhou, L. Zhou and J. Fu, *Mater. Horizons*, 2020, **7**, 1872–1882.

8 Z. Zhou, Z. He, S. Yin, X. Xie and W. Yuan, *Compos. Part B Eng.*, 2021, **220**, 108984.

9 M. Pan, M. Wu, T. Shui, L. Xiang, W. Yang, W. Wang, X. Liu, J. Wang, X. Z. Chen and H. Zeng, *J. Colloid Interface Sci.*, 2022, **622**, 612–624.

10 X. Sun, Z. Qin, L. Ye, H. Zhang, Y. U. Qingyu, W. U. Xiaojun, J. Li and F. Yao, *Chem. Eng. J.*

11 R. Wang, W. Chi, F. Wan, J. Wei, H. Ping, Z. Zou, J. Xie, W. Wang and Z. Fu, *ACS Appl. Mater. Interfaces*, 2022, **14**, 21278–21286.